CALCULATION OF THE NONSTEADY HEATING AND ABLATION OF SWOLLEN COATINGS IN HOT GAS FLOWS

V. L. Strakhov and N. G. Chubakov

UDC 539.379:536.24

Heat and mass transfer in swollen polymeric materials (PM) are studied with allowance for their thermal expansion, deformation, and chemimechanical ablation.

The use of coatings which swell intensively upon heating is a very effective method of affording protection against heat to structures operating in hot gas flows. The study [1] presented results of an investigation of nonsteady temperature fields in PM during their swelling and surface (chemical) ablation. When calculating the nonsteady heating of swollen PM-based coatings, mechanical as well as chemical ablation should be considered [by mechanical ablation, we mean the removal of parts of the coked layer (CL)]. Mechanical ablation of PM is possible as a result of the mechanical action of the gas flow, the creation of internal stresses in the material and a pressure gradient in the gases, and the occurrence of pyrolysis through the thickness of the CL. No studies have been made of the heating of swollen PM with allowance for their mechanical or chemimechanical ablation.

Proceeding on the basis of the general system of heat and mass transfer equations and dynamics of porous media, the mathematical model of the heating and ablation of swollen PM can be represented in the following form:

$$c_p'\rho'\frac{\partial T}{\partial t}=\frac{\partial}{\partial x}\left(\lambda_\Sigma(T)\frac{\partial T}{\partial x}\right)+(c_p'\rho'v'+c_p''G'')\frac{\partial T}{\partial x}-\sigma\frac{\partial\varepsilon}{\partial t}+\Pi\frac{\partial p}{\partial t}+$$

$$+\Pi(v''-v')\frac{\partial p}{\partial x}-\frac{\partial}{\partial t}\left(\frac{\rho}{1+\varepsilon}\right)\left(\frac{v''^2}{2}-\frac{v'^2}{2}\right)+Q_\Sigma\frac{\partial}{\partial t}\left(\frac{\rho}{1+\varepsilon}\right), \tag{1}$$

$$\frac{\partial\rho''\Pi}{\partial t}+\frac{\partial\rho''\Pi v''}{\partial x}=\frac{\partial}{\partial t}\left(\frac{\rho}{1+\varepsilon}\right), \tag{2}$$

$$\frac{\partial v''}{\partial t}+v''\frac{\partial v''}{\partial x}+\frac{1}{\rho''}\frac{\partial p}{\partial x}=-\frac{\Pi\mu}{k\rho''}(v''-v')-\frac{\Pi^2}{k_{ie}}(v''-v')^2, \tag{3}$$

$$\rho'\left(\frac{\partial v'}{\partial t}+v'\frac{\partial v'}{\partial x}\right)=\frac{\partial(1-\Pi)\sigma}{\partial x}-p\frac{\partial\Pi}{\partial x}-\rho'gn\cos\psi+\frac{\Pi\mu}{k}(v''-v')+\frac{\Pi^2\rho''}{k_{ie}}(v''-v')^2, \tag{4}$$

$$p=\frac{\rho''RT}{M}, \tag{5}$$

$$\varepsilon=A_\varepsilon\sigma^\beta t_{pz}^r\exp\left(-\frac{B_\varepsilon}{T}\right),\quad t_{pz}=t-t_{bp}, \tag{6}$$

$$\frac{\partial l}{\partial x}=\ln(1+\varepsilon), \tag{7}$$

$$\lambda_\Sigma=\lambda'(1-\Pi)+[\lambda''+\varkappa_{tr}(1+\varepsilon)T^3]\Pi,\quad \rho=\rho_0[1-\chi(1-K)], \tag{8}$$

$$\Pi=1-\frac{\rho}{\rho^{0\prime}(1+\varepsilon)},\quad k=k_0\frac{(K_{tr}\Pi)^3}{(1-K_{tr}\Pi)^2},\quad \rho'=\rho^{0\prime}(1-\Pi),\quad v'=\frac{\partial l}{\partial t}, \tag{9}$$

$$\chi=\begin{cases}0, & T\leqslant T_{bd},\\ A_\chi\operatorname{arctg}[\theta_\chi(T-T_{md})]+B_\chi, & T_{bd}<T<T_{ed},\\ 1, & T\geqslant T_{ed},\end{cases} \tag{10}$$

Translated from Inzhenerno-Fizicheskii Zhurnal, Vol. 55, No. 4, pp. 571-581, October, 1988. Original article submitted April 22, 1987.

0022-0841/88/5504-1103$12.50

$$0 \leqslant t \leqslant t_{\text{fin}},\ 0 \leqslant x \leqslant L_\Sigma,\ T|_{t=0} = T_0(x),\ p|_{x=x_w} = p_e,\ l_{x=x_{\text{bp}}} = 0, \tag{11}$$

$$[(1-\Pi)\sigma - \Pi p]|_{x=x_w} = p_e,\ \rho''\Pi v''|_{x=x_{\text{bd}}} = G''|_{x=x_{\text{bd}}} = 0, \tag{12}$$

$$-\lambda_\Sigma \frac{\partial T}{\partial x}\bigg|_{x=x_w} = (\alpha_w - \eta c_p'' G'')(T_e - T_w) + A_{\text{ef}}\sigma_{\text{S}}(T_e^4 - T_w^4) - G_w Q_w = q_\Sigma, \tag{13}$$

$$-\lambda_\Sigma \frac{\partial T}{\partial x}\bigg|_{x=x_{L_\Sigma}} = \alpha_{L_\Sigma}(T_{eL_\Sigma} - T_{L_\Sigma}),\ G_w Q_w = G_w^{\text{x}} Q_w^{\text{x}} + c_p'\rho'(T_w - T_0)v_w', \tag{14}$$

$$\text{Nu} = 0{,}0296\,\text{Re}_w^{0,8}\left(\frac{T_w}{T_e}\right)^{0,39}\text{Pr}_w^{0,46}\left(1 + \frac{k^*-1}{2}\text{Pr}^{0,33}M_e^2\right)^{0,11},\ M_e = \frac{v_e}{a}, \tag{15}$$

$$T|_{x=s-0} = T|_{x=s+0},\ \lambda_s \frac{\partial T}{\partial x}\bigg|_{x=s-0} = \lambda_{s+1}\frac{\partial T}{\partial x}\bigg|_{x=s+0}, \tag{16}$$

$$G_w^{\text{ch}} = \frac{\alpha b}{c_p(1-\Pi)(1-\eta_B)}\ \frac{K}{(K-m_T)},\ \Phi = \left[\left(\frac{\sigma_\Sigma}{\sigma_M}\right)^2 + \left(\frac{\tau_\Sigma}{\tau_M}\right)^2\right] = 1, \tag{17}$$

$$\sigma_\Sigma = \frac{\Pi p - p_e}{1-\Pi} + \frac{1}{1-\Pi}\int_{x_w}^{x}\rho'(gn\cos\psi + \varkappa A\omega^2)\,dx, \tag{18}$$

$$\tau_\Sigma = \frac{1}{1-\Pi}\left(\varkappa'\rho_e v_e^2 + G_{\text{cd}}v_{\text{cd}} + \int_{x_w}^{x}\rho' gn\sin\psi dx\right). \tag{19}$$

System of equations and boundary conditions (1-19) differs from the system presented in [1] in the presence of additional terms in energy equation (1). Specifically, in accordance with the first law of thermodynamics, the term $\sigma(\partial\varepsilon/\partial t)$ models the work of internal forces (mechanical stresses), which is equivalent to the losses of thermal energy due to deformation. Two other terms

$$\Pi\frac{\partial p}{\partial t} + \Pi(v'' - v')\frac{\partial p}{\partial x},\ \frac{\partial}{\partial t}\left(\frac{\rho}{1+\varepsilon}\right)\left(\frac{v''^2}{2} - \frac{v'^2}{2}\right)$$

represent the heat release associated with the work of pressure forces and the kinetic energy of the gaseous products of thermal degradation. Equations (3) and (4) also contain inertial and convective terms, as well as the inertial component of resistance $\Pi^2\rho''/k_{ie}\,(v'' - v')^2$.

A numerical estimation of the order of the above terms showed that all of them except $\sigma(\partial\varepsilon/\partial t)$ can be ignored and the problem can be solved with the assumptions made in [1].

The nonsteady nonlinear boundary-value problem of heat and mass transfer in swollen PM (1-19) was solved numerically by a finite-difference method of linearization, with refinement of the grid employed in [1, 2].

It was shown in [3] that the use of Stefan-type conditions to calculate mobile, previously unknown boundaries in ablation problems leads to the formulation of a cumbersome system of equations and corresponding conditions. In connection with this, the problem is difficult to solve in general form because it not only entails a large amount of computation, but also involves a large number of unknown characteristics and parameters. Both chemical and mechanical ablation occur on PM in gas flows [4], this ablation being connected with the destruction of material by mechanisms [such as that corresponding to the second equation of (17)] which cannot be described with Stefan-type conditions. Thus, to calculate mobile unknown boundaries in problems of this class (i.e., to calculate boundaries formed in the mechanical, chemical, or chemimechanical ablation of swollen PM in gas flows), investigators have developed algorithms which employ implicit conditions for the appearance of such boundaries [including conditions of the form (17)]. These conditions include the limiting stresses, disintegration temperature, and other characteristics. The positions of mobile PM boundaries during chemical ablation was calculated by an algorithm similar to that described in [5]. To calculate mechanical ablation of a PM by the von Mises – Hill criterion [the second condition of (17)], we developed an algorithm based on movable grids. In accordance with [6], we calculate the distance S^m that can be travelled by the boundary $x = \xi(t)$ as follows:

$$t = t_{n+k},\ S^m = \xi(t_{n+k}) - \xi(t_n) =$$

$$= \begin{cases} \sum\limits_{i=j^n+1}^{j_d^m} h_i^m + x_d^*,\ \Phi(x_j^*) = 1,\ j^m = j^n + d^m, \\ \sum\limits_{i=j^n+1}^{j_l^m} h_i^m + x_d^*,\ (\Phi(x_l^*) > 1) \cap T(x_l^*,\ t) = T_{ep}),\ j^m = j^n + l^m. \end{cases}$$

Here, we examined two possible variants of satisfaction of condition (17): when ablation occurs in an arbitrary section $x = x_d^*$ (the CL or the degradation zone DZ ($T_{bd} \le T \le T_{ed}$)) (first determination of S^m) and when separation of the layers of degraded material occurs in the weakest section of the DZ $x = x_\ell^* = x_{ep}$ (second determination of S^m).

Then the position x^m of the mobile boundary can be determined as follows:

$$t_D = t_{n+k} - t_n,\ x^m = x^n + S^m,\ L_\Sigma^m = L^n - S^m,\ v^m = \frac{S^m}{\tau_m},\ m = n + k,$$

$$x_0^{n=0} = 0,\ x_I^{n=0} = L_\Sigma^0,\ i = 0,\ 1,\ \ldots,\ I,\ j^m < I,\ j^{n=0} = 0,\ d^m \neq l^m,$$

$$d,\ l,\ k = 1,\ 2,\ \ldots,\ n = 0,\ 1,\ \ldots,\ N,\ t_{n=0} = 0,\ t_{n=N} = t_{fin}.$$

Here, t_D is the period of displacement of the boundary (the time interval separating two successive movements of the boundary); h and τ are the spacings of the grid with respect to x and t; i and n are the numbers of the grid nodes with respect to the space coordinate and time; j^m is the number of nodes for which the condition $x_j^m < x^m$ is satisfied, i.e., the number of nodes in the separated layer of degraded material; m, z, ℓ, and d are auxiliary symbols.

After the displacement of the mobile boundary (ablation of the PM – part of the CL), the following operations are performed for the remaining (I – j) nodes of the difference grid. The mesh of the new grid region is calculated from the relations

$$\Delta h_i^m = \frac{\Delta x}{z},\ z = I - j,\ \Delta x = \begin{cases} x_d^*,\ \Phi(x_d^*) = 1, \\ x_l^*,\ (\Phi(x_l^*) > 1) \cap (T(x_l^*,\ t) = T_{ep}), \end{cases}$$

$$h_i^m = h_i^m - \Delta h_i^m,\ i = j + 1,\ \ldots,\ I,\ j = j_d \cup j_l.$$

The values of the functions at the resulting (after displacement of the boundary by S^m) nodes are determined with suitable interpolation formulas from the values of these functions at the "old" (before the displacement of the boundary) nodes:

$$T(x_w^m,\ t) = T(x^m,\ t),\ T(x_i^m,\ t) = T(x_i^n + \Delta x_i^m,\ t),$$

$$\Delta x_i^m = h_i^m - h_i^n + \Delta x_{i-1}^m,\ \Delta x_{i=jm} = \Delta x,\ h_i^{n=0} = h_{i0},$$

$$i = \begin{cases} j_d^m + 1,\ \ldots,\ I,\ \Phi(x_d^*) = 1, \\ j_l^m + 1,\ \ldots,\ I,\ (\Phi(x_l^*) > 1) \cap (T(x_l^*,\ t) = T_{ep}). \end{cases}$$

Heat and mass transfer in swollen PM were studied on a computer with the use of a program written in FORTRAN to perform parametric calculations [5]. Here, we studied the effect of deformation (curves 1 and 3 in Figs. 1 and 2), the loss of thermal energy in deformation (curves 2, 3, 6, 7 in Figs. 1 and 2), the intensity of deformation (curves 4 and 5 in Fig. 2), and total ablation (Figs. 1 and 2 show data without allowance for ablation, Figs. 3 and 4 show data with allowance for ablation) on heat and mass transfer. The inverse effect was also calculated (curves 8 and 9 in Fig. 2).

The main computational variant (curve 3 in Figs. 1 and 2, curves 1 and 2 in Figs. 3 and 4 – with allowance for deformation (swelling) and loss of heat energy due to deformation) was calculated for a rubberlike PM based on phenol-formaldehyde resin binder. The characteristics of the PM, determined by a method similar to that used in [1], were as follows: T_e = 3500 K; $\kappa_{tr} = 4 \cdot 10^{-11}$ W/(m·K); A_{ef} = 0.55; b = 0.12; τ_M = 430 Pa; T_0 = 293 K; $c_p'' = 5 \cdot 10^3$ J/(kg·K); $\rho' = 1500$ kg/m³; $\lambda_1' = 0.3$ W(m·K); $T_{bp} = T_{bd} = 550$ K; $T_{ed} = 1100$ K; $Q_\Sigma = 10^6$ J/kg; $B_\varepsilon = 1.5 \cdot 10^3$ K;

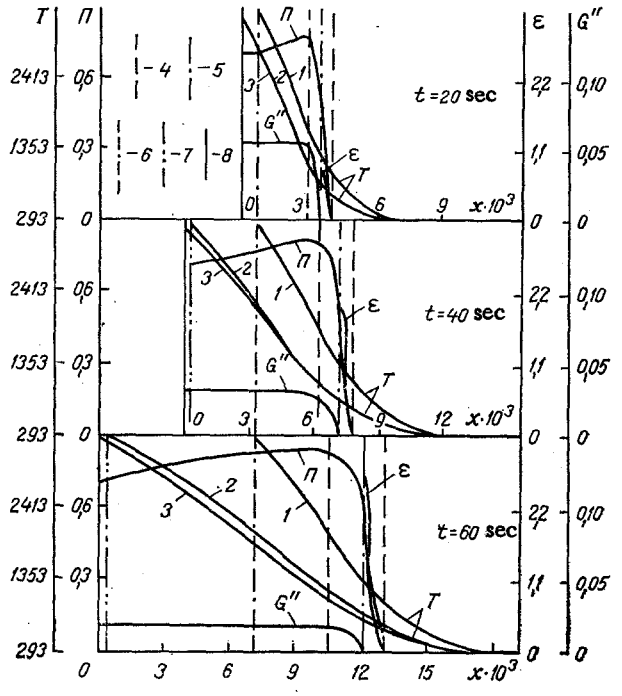

Fig. 1. Distribution of temperature and the mass rate of filtration of gaseous products of thermal degradation of the binder, porosity, and deformation over the thickness of the swollen PM and time: 1) $\varepsilon = 0$; 2) $\varepsilon \neq 0$, $\gamma = 0$, $\gamma = \sigma(d\varepsilon/dt)$; 3) $\varepsilon \neq 0$, $\gamma \neq 0$; 4) DZ; 5) PZ; 6, 7, 8) position of the heated surface of the PM for conditions 1, 2, and 3, respectively. T, K; G", kg/(m²·sec); x, m.

M = 50 kg/kmole; s = 1.2; $\alpha_{L\Sigma} = 0$ W/(m²·K); $\lambda_2 = 0.2$ W/(m·K); $c_{p^2} = 1450$ J/(kg·K); $\rho_2 = 1400$ kg/m³; h = 10^{-5}-$2\cdot10^{-4}$ m; $x = x_d^*$; $t_{fin} = 60$ sec (parameters not indicated in the figures or in the captions correspond to the main variant). Calculations were performed for a two-layer plate, the first layer of which was swollen. We examined the most typical case, when the DZ includes the zone of plastic deformation PZ ($T_{bp} \leq T \leq T_{ep}$), i.e., $T_{bd} \leq T_{bp} < T < T_{ep} < T_{ed}$.

Figures 1 and 2 show the results of study of heat and mass transfer in a swollen PM without allowance for the total chemimechanical surface disintegration. The character of change in the deformation and porosity of the PM (Figs. 1 and 2) is identical to that established in [1]. The mass rate of filtration (transport) of the gaseous products of thermal degradation of the polymer binder has a maximum on the boundary between the DZ and CL (Fig. 1). The values of filtration rate decrease with time, while the values of porosity increase. This occurs because deformation – which affects both mass transport and pore formation [see (2) and (9)] – increases over time, as can be seen from Figs. 1 and 2. The latter fact can be explained by the fact that the rate of advance of the DZ decreases with time – for the depth of thermal degradation δ we have $\dot{\delta} = \partial\delta/\partial t \sim 1/\sqrt{t}$. Thus, each given elementary volume of material spends more time in the PZ than the preceding volume. Swelling plays an important role in the pore formation process in that porosity increases significantly near the internal boundary of the CL (Fig. 1, t = 60 sec).

Deformation of the PM leads to straightening of the temperature profile in the material due to an increase in its volume (which reduces the temperature gradient). Deformation also leads to a reduction in heat conduction due to an increase in porosity, which causes "blocking" of the process of heat propagation (a reduction in heating rate). Thus, the temperature at the point $x = L_0/2$, which is fixed relative to the boundary between the first and second layers (x = L), decreases in the first 60 sec (Fig. 1) from ~900 K (curve 1, without allowance for swelling) to ~585 K (curve 3), or by a factor of ~1.55. With a reduction in the rate of swelling (for example, with a 100% increase in the molecular weight of the gaseous degradation products), the temperature at this point decreases by a factor of ~1.5 (curves 1 and 5 for T in Fig. 2). With an increase in swelling rate (for example, with a reduction in pressure to $p_e = 0.1$ MPa), this temperature decreases by a factor of two (curves 1 and 4 for T, Fig. 2).

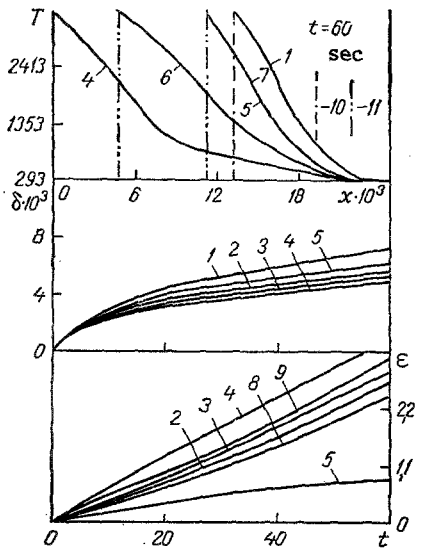

Fig. 2

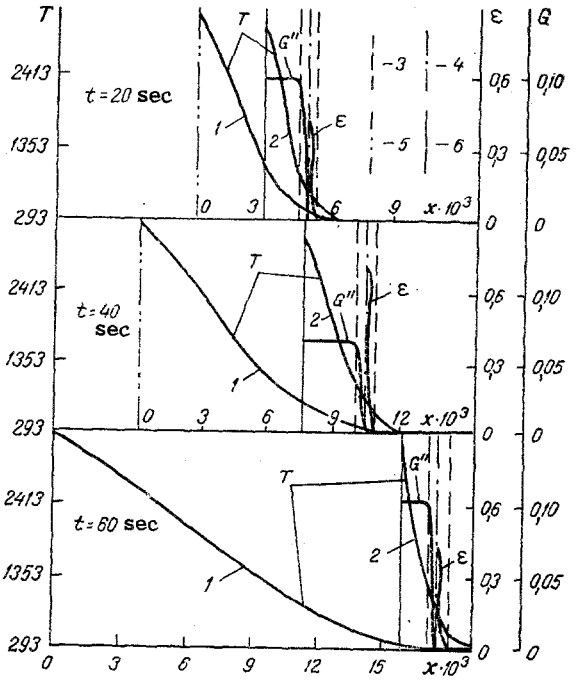

Fig. 3

Fig. 2. Profile of temperature through the thickness and dependence of the depth of degradation δ and the deformation of the PM on time: 1) $\varepsilon = 0$; 2) $\varepsilon \neq 0$, $\gamma = 0$; 3) $\varepsilon \neq 0$; 4) $p_e = 0.1$ MPa; 5) M = 100 kg/kmole; 6) $p_e = 0.1$ MPa, $\gamma = 0$; 7) M = 100 kg/kmole, $\gamma = 0$; 8) $q = 150\%\ q_\Sigma$; 9) $q = 50\%\ q_\varepsilon$; 10, 11) position of the surface of the PM for 1; (4, 6) and (5, 7), respectively. δ, m; t, sec.

Fig. 3. Profiles of temperature, the mass rate of filtration of gaseous thermal-degradation products, and deformation through the thickness of the PM at different moments of time: 1) $G_{di} = 0$; 2) $G_{di} \neq 0$; 3) DZ; 4) PZ; 5, 6) position of the surface of the PM for conditions 1 and 2, respectively.

Thus, swelling of the PM reduces the rate of heat transfer by a factor of 1.5-2 (or more, depending on the rate of swelling).

Figures 1 and 2 (curves for T) show the effect of heat loss on deformation – allowing for these losses leads to a reduction in the rate of heat transfer (the size of this reduction being determined by the rate of swelling) and to an intensification of swelling. Thus, over 60 sec, the temperature at a point which is fixed relative to the boundary of the first and second layers ($x = L$) $x = (2/3)L_0$ (Fig. 1) is reduced from ~950 K to ~855 K (curves 2 and 3, respectively), i.e., by ~9%, while the increase in thickness is ~2%. With an increase in swelling rate (temperature curves 4 and 6 in Fig. 2), the temperature at this point (the region DZ) is reduced by ~25%. In the region of the original, undegraded PM (at the point $x = L_0/2$), the temperature reduction is ~14%. The increase in thickness is ~17%. Thus, calculating heat transfer in a PM without allowance for heat loss due to deformation leads to overstatement of temperature for the entire PM: by up to ~25% in the DZ (and more in the CL – see curves 4 and 6 for T in Fig. 2); up to ~16% in the layer of original material (or more, depending on the swelling rate). The study established that calculation of the heating of a PM in hot gas flows without consideration of energy loss due to deformation also leads to exaggeration of mass transfer (filtration) by 20-30%. It is evident from Fig. 2 (temperature curves 5 and 7) that the effect of energy loss due to deformation is negligible (with temperature reduction amounting to ~0.1%) only in the event of a substantial decrease in swelling rate (such as due to an increase in the molecular weight of the gaseous mixture of degradation products). This means (and has been proven by calculations) that these losses can be ignored only in the case of relatively small deformations of the PM (such as with an extension $K_L = (L/L_0) < 1.4$).

Swelling decreases the depth of degradation of the material by ~20% (curves 1 and 3 in Fig. 2). At high swelling rates, swelling reduces the depth of degradation by ~28% (curves 1, 4), leading to a decrease in heat flow in the second layer of the plate. Analysis of

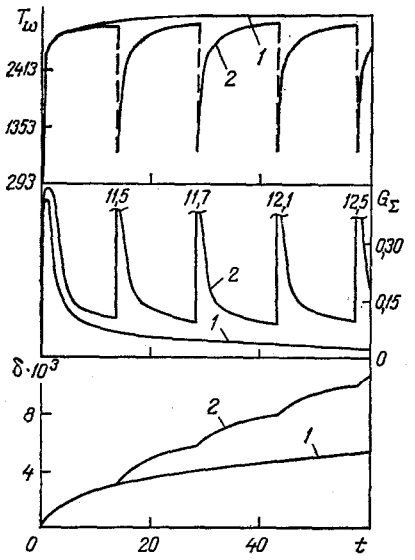

Fig. 4. Time dependence of the temperature of the surface of the PM, the total mass rate of disintegration, and the depth of degradation: 1) $G_{di} = 0$; 2) $G_{di} \neq 0$.

curves 2 and 3 for δ (Fig. 2) shows that when the heating of a PM in gas flows is calculated without allowance for the energy loss to deformation, degradation depth is increased by ~5.5% (or more, depending on the rate of deformation – as is evident from temperature curves 4 and 6).

Figure 2 shows the effect of heat transfer on swelling rate (curves 3, 8, and 9 for the deformation). A change in the heat flux to the PM by amounts of up to 50% (curves 8 and 9, respectively) changes the deformation by −14% and +7%, respectively (compared to curve 3). Thus, the reduction in deformation that occurs with an increased heat flux is more than twice as great as the increase in deformation that occurs with a reduced heat flux. This result is attributable to the fact that the PZ moves more rapidly into the PM with an increase in heating rate (or, alternatively, the degradation depth increases more rapidly), so that the time during which an elementary volume of material is in this zone is reduced.

Figures 3 and 4 show the results of study of heat and mass transfer in a swollen PM in the event of its complete surface disintegration – with chemical (in the diffusion regime) and mechanical (by the von Mises–Hill criterion) ablation [Eqs. (17), respectively]. The figures also show the results obtained with allowance for the entrainment of the gaseous products of thermal degradation of the binder that are given off inside the PM and filter to the permeable surface of the material through pores in the CL (i.e., $G_\Sigma = G_w' + G_w'' + G_w^{ch}$, $v_\Sigma = v_w' + v_w'' + v_w^{ch}$).

To explain the effect of chemimechanical ablation (leading to a change in the dimensions of the PM), we compared the results obtained with fixed boundaries (curves 1 in Figs. 3 and 4) against the results of calculations with movable external boundaries (curves 2 in the same figures). Here, $G_{di} = G_w' + G_w^{ch}$. The rate of ablation of the PM is greater than the rate at which it swells. Deformation of PM and its internal disintegration (thermal degradation of the binder, filtration and injection of gaseous degradation products) were considered in both of the computational variants being compared.

Complete surface disintegration of a swollen PM leads to an intensification of heat transfer, since the temperature at the boundary $x = L$ at $t = 60$ sec increases from ~293 K (curve 1 in Fig. 3 – without allowance for ablation) to ~360 K (curve 2), i.e., by ~20%. However, under conditions of intensive complete ablation, the PM still does not reach the temperature corresponding to the beginning of degradation, due to "blocking" of the heat propagation process with swelling.

It was established that the effect of the loss of heat energy on the processes of heat and mass transfer and pore formation in the PM, the depth of its degradation, the change in thickness, etc. is negligible, as is its effect on the character of the time and space distributions of temperature, porosity, mass rate of disintegration, etc., during intensive ablation.

It follows from an analysis of the curves in Fig. 3 that during ablation of a PM, the change in the maximum rate of filtration of gaseous degradation products and the maximum de-

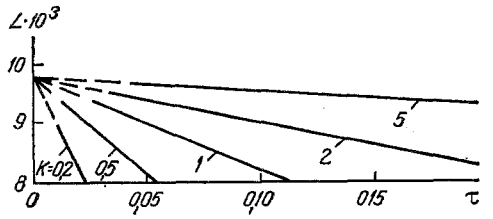

Fig. 5. Dependence of the running thickness of a swollen PM on the grid parameters h and τ for different ratios of these parameters, characterized by the Curant number K. L, m.

formation of the material over time is nonmonotonic in character, in contrast to their monotonic change in the absence of surface disintegration (Fig. 1). This is due to the fact that the values of deformation in the remaining (after ablation of part of the CL) material are lower, since the time an elementary volume of material spends in the PZ is reduced (as follows from Fig. 3) due to the more rapid advance of the DZ during ablation. This is the reason that porosity also changes nonmonotonically with respect to both time and the space coordinate, while its values in the presence of ablation are lower than in the case of a fixed external boundary for the PM.

The dependence of the temperature of the surface of a swollen PM on the time of heating during its complete surface disintegration is "saw-toothed" in form (curve 2 for T_w, Fig. 4). It has this form because periodic separations (ablation) of parts of the CL result in temperature discontinuities – the surface temperature first suddenly decreases and then again increases. In the disintegration of a swollen PM, its surface temperature declines by ~6.2% compared to the variant in which the external boundary is fixed (curve 1 for T_w, Fig. 4). The reduction in temperature is due to the fact that surface disintegration involves ablation, leading to displacement of the surface into parts of the CL with a lower heat content, i.e., into "colder" sublayers of the CL.

It is evident from curve 2 for G_Σ in Fig. 4 that along with the extremum in the initial period, the dependence of the mass rate of disintegration on heating time has additional extrema corresponding to individual moments of disintegration (separation of sublayers) of the CL. The presence of the extrema can be attributed to the fact that ablation is accompanied by an increase in the quantity of gaseous products, since the remaining, less heated material (with a lower heat content) is subjected to more intensive heating. The separation of the sublayers of the CL during mechanical disintegration also helps account for the extrema. As was established from the study result, for this reason the flow rate of gaseous degradation products increases by 50-70% with surface disintegration. The numbers near curve 2 for G_Σ in Fig. 4 correspond to values of the instantaneous rate of mechanical ablation. Curve 1 shows the total rate of chemical ablation and the rate of removal of gaseous degradation products.

The increase in these values over time is due to the reduction in porosity which accompanies surface disintegration (the rate of which exceeds the swelling rate). Thus, in accordance with (18), the stresses necessary for the disintegration of the CL will be reached at a greater depth after each successive separation of a CL sublayer, which will in turn result in an increase in the depth of the thickness of the sublayer that is removed (an increase in the instantaneous rate). Analysis of the change in the running size of the PM (see Fig. 3) and its rate of disintegration G_Σ (Fig. 4) shows that mechanical ablation plays the main role in the surface disintegration of the material.

The complete surface disintegration of a swollen PM causes an increase in depth of its degradation by ~50% (curves 1 and 2 for δ, Fig. 4, t = 60 sec). The time dependence of the degradation depth has a stepped character due to the fact that, with mechanical ablation (separation of part of the CL), the rate of displacement of the DZ increases rapidly.

According to the data in [1], with chemical ablation of a PM, there is a substantial reduction in the degradation depth – the reduction depending on the rate of swelling. Numerical experiments established that with complete (chemimechanical) surface disintegration (at one rate) of a swollen PM, the degradation depth is shallower than for an unswollen material (heating of the latter to the temperature corresponding to the end of degradation begins considerably more rapidly).

Comparison of calculated results [1] with experimental data for a swollen PM shows that they agree well. Following [6], we also conducted a special numerical study of the convergence of difference solutions of model (1-19). The results of the study, confirming the convergence of the numerical solutions to the corresponding differential solutions, are shown

in Fig. 5. Thus, both the agreement between the theoretical and experimental results and the convergence of solutions obtained by different computational methods show that the method described here is reliable and that model (1-19) adequately reflects the process of heat and mass transfer in a swollen PM.

The results of the above investigation show that deformation and the associated loss of energy have a significant effect on heat and mass transfer, pore formation, and other processes in a PM. However, the results also demonstrate the superior properties of a swelling PM compared to a nonswelling material, since degradation depth is considerably shallower in the former even under conditions of intensive surface disintegration. In connection with this, it is preferable to use swelling materials, since they are more reliable than conventional materials.

NOTATION

t, x, L, time, coordinate, thickness; T, λ, q, temperature, thermal conductivity, heat flux; c_p, Q, heat capacity, thermal effect; ρ, v, density, velocity; Π, G, porosity, mass rate; σ, τ, normal and shear stresses; ε, p, deformation, pressure; μ, k, k_{ie}, absolute viscosity and permeability (viscous and inertial); g, n, ψ, acceleration due to gravity, overload, angle between the normal and the inertial force line; κ, A, ω, dynamic coefficient, amplitude, and frequency of vibrations; R, M, universal gas constant and molecular weight; A_ε, B_ε, parameters of the kinetics of deformation; ℓ, K, K_{tr}, displacements, coke number (or Curant number), transmittance; A_χ, Θ_χ, B_χ, parameters of the kinetics of thermal degradation (breakdown, pyrolysis, depolymerization); α, η, heat-transfer and injection coefficients; A_{ef}, σ_s, function of the radiative properties of the gas and surface, Stefan–Boltzmann constant; κ_{tr}, κ', parameter of radiative heat transfer in pores, resistance coefficient of surface projections; b, m_I, η_B, oxidation potential, mass fraction of filler in the initial material and material of the CL subjected to chemimechanical breakup, determined from [4]; k*, a, adiabatic index, speed of sound; β, r, exponents. Indices: 0, initial, Σ, total; bd, md, ed, beginning, maximum, and end of thermal degradation; bp, ep, beginning and end of plastic deformation; e, gas flow; w, heated surface of the PM (interacting with the gas flow); s, number of the layer; M, limiting value of the parameter accounting for motion of the boundaries (with ablation of the PM); cd, condensed phase; fin, final; di, disintegration; ^{0}, monolithic (without pores); ', ", solid and gas phases; ch, chemical ablation.

LITERATURE CITED

1. V. L. Strakhov and N. G. Chubakov, Inzh.-Fiz. Zh., 45, No. 3, 472-479 (1983).
2. N. G. Chubakov and G. V. Kuznetsov, Inform. Bulletin Gos. FAN: Algorithms and Programs, Moscow (1982), No. 7, pp. 63-64.
3. G. A. Tirskii, Zh. Vychisl. Mat. Mat. Fiz., 1, No. 5, 884-902 (1961).
4. B. M. Pankratov, Yu. V. Polezhaev, and A. K. Rud'ko, in: Interaction of Materials with Gas Flows [in Russian], Moscow (1975), pp. 183-190.
5. V. L. Strakhov and N. G. Chubakov, Inzh.-Fiz. Zh., 47, No. 4, 677-678 (1984).
6. N. G. Chubakov, Inzh.-Fiz. Zh., 42, No. 3, 491-492 (1982).